Response

Comments to the Author:

The presented manuscript proposes a comparison, in the context of the use of compositional data analysis (CoDA) techniques to perform digital soil mapping of particle-size fractions, of different ILR transformation choices and different prediction algorithms. The authors, after having provided a brief analysis of the current literature on the use of compositional data in geosciences, they perform three different ILR transformations of the data, and then proceed to assess sat comparing the prediction accuracy of several statistical learning methods, namely linear regression (glm with gaussian errors and identity link is classical least squares, gaussian regression), universal kriging and random forests, via the use of a real world dataset. They then conclude by assessing what is the best algorithm in terms of prediction by inspecting several performance metrics. While I do think that the general topic of investigation is of quite interest for an audience of geosciences practitioners, and so it is coherent with the aims of this Journal, I am quite concerned by the execution of the paper, and I think some very serious points need to be tackled before this paper is able to be considered suitable for publication:

Comment 1. The wording is very obscure at times, hindering the very comprehension of the matters at hand.

Response: Thanks for the suggestion about the quality of the English language of this paper. We looked for some senior editors from a professional English polishing company to improve the overall language of this article and we have checked and improved the writing in the revised version.

Charlesworth
Author Services

EDITORIAL CERTIFICATE

This document certifies that the manuscript below was edited for correct English language usage, grammar, punctuation and spelling by qualified native English speaking editors at Charlesworth Author Services.

Paper Title：

Compositional balance should be considered in soil particle-size fractions mapping using hybrid interpolators

Author:
Wenjiao Shi

Date certificate issued:

Nov. 23, 2020

cwauthors.com

18

Comment 2. Judging by how the performance metrics are chosen, the prediction problems solve by the authors are all scalar ones, and so the methods seem to having been applied separately to the different components. This is wrong, as it is fundamental in a compositional setting to inspect the cross-correlations between variables (and thus use multivariate prediction methods).

Response: For the performance metrics, the Aitchison Distance (AD) was applied as an indicator to evaluate the overall performance of the models. The AD can consider a multivariate setting. In addition, we also wanted to evaluate and compare which component (i.e., sand, silt, and clay) performed best among these prediction models. In the field of soil PSF spatial prediction, each component should be evaluated and not just the overall impact, which will help to fully understand the modeling process. The three ILR balances produced different ILR data, with distinct data ranges and other statistical characteristics. This is why we explored whether different balances would affect one soil PSF component and further improve the accuracy.

We think that correlations among the components (i.e., sand, silt, and clay) can be revealed using an ILR transformation. Therefore, the models considered the joint fractions by transforming the original soil PSF data from simplex (three components) to the real space (two ILR components). Moreover, the reason why we predicted each ILR component separately is because that was a more suitable approach for the spatial prediction models currently used (such as the GLM and RF). In general, in the formula for a single prediction model (GLM and RF), only one column of observations (ILR1 or ILR2) is included, generating one column of predictions. Therefore, these models cannot consider multiple variables (observations, ILR1 and ILR2) together in one formula. Some previous studies (Akpa et al., 2014; Buchanan et al., 2012; Huang et al., 2014; Nagra et al., 2017) have used similar methods in combination a with log-ratio transformation to make predictions of soil PSF in other study areas, and we think our results can therefore provide guidance for other studies. For the multivariable methods, we have used compositional kriging for the spatial prediction of soil PSFs in our previous studies (Wang and Shi, 2017, 2018); however, this approach cannot be combined with environmental covariables to achieve one of the objectives of this work, i.e., using hybrid interpolation. For the other models, a multivariate RF may be an alternative method for considering multivariate settings in future research. We have improved this part of the paper in the revised version (Discussion **4.3 Limitations**)

P21L538: 4.3 Limitations.

"In this work, we used ILR transformation to demonstrate the correlation of soil PSF data, and different balances were also compared. However, these models were predicted separately for each ILR component (ILR1 and ILR2), which were suboptimal because they cannot further consider the cross correlations among ILR coordinates. In our pervious study, we have used compositional kriging (CK) for the spatial prediction of soil PSFs (Wang and Shi, 2017), and the cross correlations of ILRs can be taken into account using CK. Although it is optimal, it cannot consider different balances of ILR, nor can it be combined with the hybrid interpolator (e.g., RK). Moreover, predicting each ILR component separately was a more suitable approach for the spatial prediction models currently used (such as the GLM and RF). Therefore, more alternative spatial prediction models combined with interpretation of ILR balances for compositional data should be considered in the future. For example,

CK and high accuracy surface modelling (HASM; Yue et al., 2016) can be applied for small scale study areas. For large scale study areas, multivariate RF (Segal and Xiao, 2011) can be combined with a log-ratio transformation and hybrid interpolation, enabling the cross correlations among ILR coordinates to be better interpreted."

Refrence

Akpa, S. I. C., Odeh, I. O. A., Bishop, T. F. A., and Hartemink, A. E.: Digital Mapping of Soil Particle-Size Fractions for Nigeria, Soil Sci. Soc. Am. J., 78, 1953-1966, 10.2136/sssaj2014.05.0202, 2014.

Buchanan, S., Triantafilis, J., Odeh, I. O. A., and Subansinghe, R.: Digital soil mapping of compositional particle-size fractions using proximal and remotely sensed ancillary data, Geophysics, 77, WB201-WB211, 10.1190/geo2012-0053.1, 2012.

Huang, J., Subasinghe, R., and Triantafilis, J.: Mapping Particle-Size Fractions as a Composition Using Additive Log-Ratio Transformation and Ancillary Data, Soil Sci. Soc. Am. J., 78, 1967-1976, 10.2136/sssaj2014.05.0215, 2014.

Nagra, G., Burkett, D., Huang, J., Ward, C., and Triantafilis, J.: Field level digital mapping of soil mineralogy using proximal and remote-sensed data, Soil Use Manage., 33, 425-436, 10.1111/sum.12353, 2017.

Segal, M. and Xiao, Y. Y.: Multivariate random forests, Wiley Interdisciplinary Reviews-Data Mining and Knowledge Discovery, 1, 80–87, https://doi.org/10.1002/widm.12, 2011.

Yue, T., Liu, Y., Zhao, M., Du, Z., and Zhao, N.: A fundamental theorem of Earth's surface modelling, Environ. Earth Sci., 75, 751, https://doi.org/10.1007/s12665-016-5310-5, 2016.

Wang, Z., and Shi, W. J.: Mapping soil particle-size fractions: A comparison of compositional kriging and log-ratio kriging, J. Hydrol., 546, 526-541, 10.1016/j.jhydrol.2017.01.029, 2017.

Wang, Z. and Shi, W.: Robust variogram estimation combined with isometric log-ratio transformation for improved accuracy of soil particle-size fraction mapping, Geoderma, 324, 56–66, https://doi.org/10.1016/j.geoderma.2018.03.007, 2018.

Comment 3. Given that linear methods (such as linear regression and regression kriging) are invariant to the choice of ILR basis, I am baffled by seeing results for these methods that are different across different ILR transformation.

Response: For the same soil sampling point within the soil PSF raw data, different ILR balances produced different ILR values (ILR1 and ILR2). There is no doubt that they can be back-transformed with the same values of soil PSFs (sand, silt, and clay) even though the balances were different (Fig. 1). For the soil PSF interpolation, the raw data first transformed the ILR mode (two components of ILR1 and ILR2), then interpolated and finally back-transformed to the raw data form (three components of sand, silt, and clay). Using three SBPs resulted in different input values for the interpolation, and also produced different results. Therefore, for soil PSFs the ILR balance should be selected carefully.

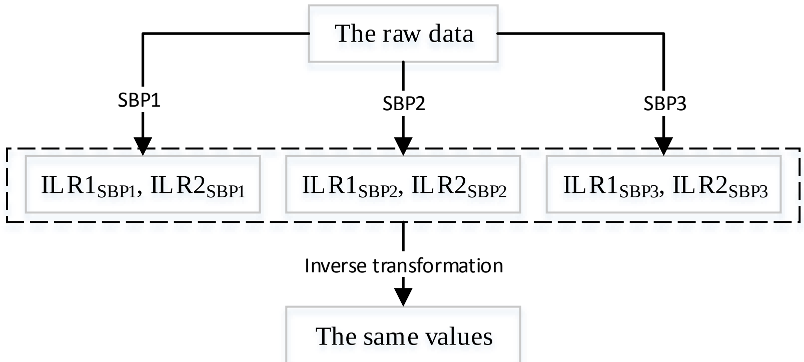

Fig. 1. Transformation and inverse transformation of ILR methods based on different SBPs.

Different GLM and GLMRK models based on three ILR balances generated different results in our study, but this is not indicating that choosing the ILR basis has the influence on the results themselves. We find that there are four aspects causing the difference in our prediction results when we check the process and code we used: (1) the environmental covariables applied for each prediction model; (2) the predicted ILR components of the testing sets; (3) the back-transformed values for the three components of soil PSFs; and (4) the predicted ILR residuals (testing sets) without back transformation (only for the RK method).

For (1). The three ILR balances generated different transformed datasets. The GLM model used the "glmStepAIC" algorithm (i.e., a stepwise regression) to select the best combination of environmental covariables for each ILR component. (**P8L314** *"The Akaike's information criterion (AIC) was applied to choose the best predictors and remove model multicollinearity using a backward stepwise algorithm."*) Therefore, the variable inputs were different for these ILR data. We listed the choice of variables of each ILR for one random prediction (Table 1).

Table 1. Combination of environmental covariables for different ILR data.

Data	Combination of environmental covariables
ILR1SBP1	WWC + ndvi + lon + soc + rain + CNB + NH
ILR2SBP1	FWHC + WWC + ndvi + tem + soc + dem + rain + AHS + aspect + MSP
ILR1SBP2	FWHC + WWC + ndvi + tem + soc + SHC + dem + rain + AHS + aspect + MSP
ILR2SBP2	FWHC + WWC + lon + soc + aspect + CNB + MSP + MRVBF
ILR1SBP3	FWHC + WWC + tem + lat + soc + dem + aspect + CNB + MSP + MRVBF
ILR2SBP3	ndvi + tem + soc + SHC + dem + rain + aspect + MSP + SH

For (2) and (3). Moreover, an independent dataset validation was used for the accuracy assessment in this study. The training and testing sets were entirely different and had no intersection. Therefore, the predicted ILRs in the testing sets were different and the back-transformed soil PSFs and the accuracy indicators (ME and RMSE) were also different.

For (4). For the validation and prediction maps of RK, the results were the sum of the predicted ILR and ILR residuals, which were then back-transformed, producing different values (Fig. 2). We also noticed that although the differences among the values were small, the inverse transformation can enlarge the difference and prediction errors because of the value ranges.

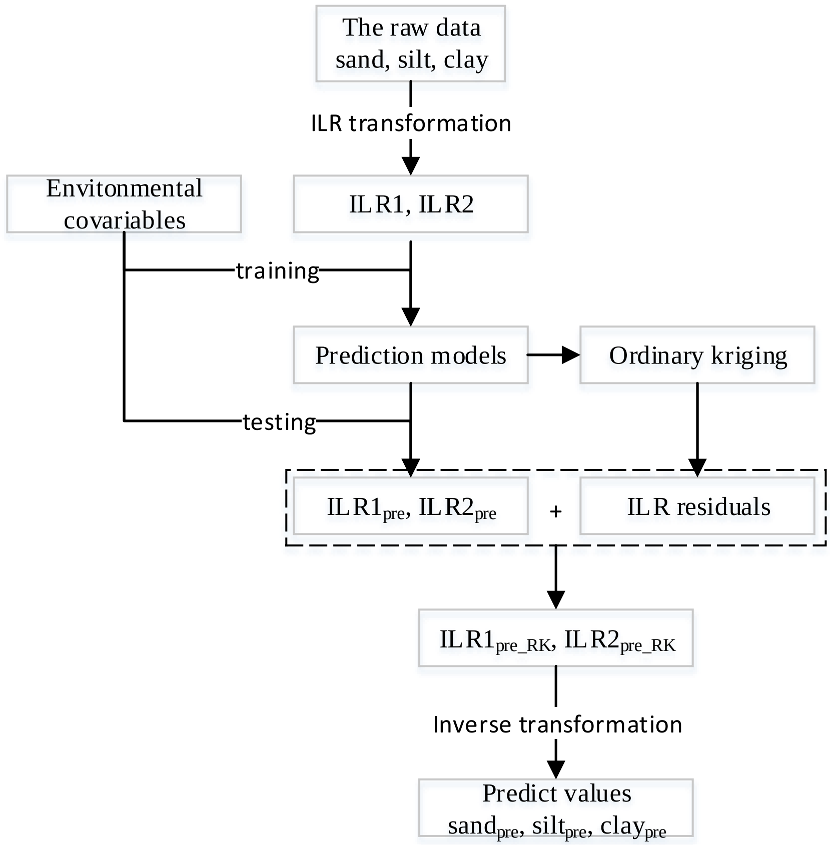

Fig. 2. Process of RK method in our study.

In summary, we think the reasons for the different results start with the first step (EC selection), and affect the next steps. We have added more explanation for this in our revised version.

P20L503: *"The results of GLM and GLMRK should not depend on the ILR basis being chosen, which has been proved by previous studies on the use of linear models and kriging for compositional data (Pawlowsky-Glahn et al, 2015). However, the GLM model used the "glmStepAIC" algorithm (i.e., a stepwise regression) to select the best combination of environmental covariables for each ILR component. Therefore, the variable inputs were different for these ILR data, and further impact the accuracy assessment and prediction maps."*

Reference

Pawlowsky-Glahn V, Egozcue JJ, Tolosana-Delgado R.: Modeling and analysis of compositional data. John Wiley & Sons, Ltd, 2015.

Comment 4. The estimation of a bias metric via the use of RMSE on unbiased estimators (such as LM and RK) is simply incorrect.

Response: We agree that the linear models and RK are unbiased. However, in the validation method used in this study, an independent dataset validation was used for the accuracy assessment. Therefore, the training (70%) and test (30%) sets were entirely different and had no intersection. Although these models are unbiased, we can also verify the bias of an independent dataset (predictions) using the mean error (ME). In other words, for spatial interpolation, the usual methods of validation for comparing the interpolation methods are known as cross-validation and validation with an independent data set. Cross-validation involves eliminating each observation in turn, estimating the value at its site from the remaining observations and comparing the predicted value with the measured value. This procedure is a rapid, inexpensive one for comparing predicted and measured values. Unfortunately, it has limitations in many cases. For kriging estimators, it retains the same variogram, and to be true cross-validation the variogram should be recomputed and fitted afresh when each observation is removed. These shortcomings can be avoided by using an independent data set for validation. Validation with an independent data set which is a superior and more dependable method directly estimates the spatial uncertainty, as validation points are located randomly throughout the field (Shi et al., 2009). Therefore, the concept of unbiased is for all sampling points, not for the validation.

We have listed some previous studies that used ME to evaluate soil PSF prediction bias for a linear regression (LR) method combined with a log-ratio, which confirms that the use of these univariate metrics should not be avoided (Buchanan et al., 2012; Huang et al., 2014).

Refrence

Buchanan, S., Triantafilis, J., Odeh, I. O. A., and Subansinghe, R.: Digital soil mapping of compositional particle-size fractions using proximal and remotely sensed ancillary data, Geophysics, 77, WB201-WB211, 10.1190/geo2012-0053.1, 2012.

Huang, J., Subasinghe, R., and Triantafilis, J.: Mapping Particle-Size Fractions as a Composition Using Additive Log-Ratio Transformation and Ancillary Data, Soil Sci. Soc. Am. J., 78, 1967-1976, 10.2136/sssaj2014.05.0215, 2014.

Shi, W., Liu, J., Du, Z., Song, Y., Chen, C., and Yue, T.: Surface modelling of soil pH, Geoderma, 150, 113-119, 10.1016/j.geoderma.2009.01.020, 2009.

Special thanks to you for your kind comments.

Yours sincerely,

Wenjiao Shi

E-mail: shiwj@lreis.ac.cn

Compositional balance should be considered in the mapping of soil particle-size fractions~~ mapping~~ using hybrid interpolators

Mo Zhang[1,2], Wenjiao Shi[1,3]

[1]Key Laboratory of Land Surface Pattern and Simulation, Institute of Geographic Sciences and Natural Resources Research, Chinese Academy of Sciences, Beijing 100101, China
[2]School of Earth Sciences and Resources, China University of Geosciences, Beijing 100083, China
[3]College of Resources and Environment, University of Chinese Academy of Sciences, Beijing 100049, China

Correspondence to: Wenjiao Shi (shiwj@lreis.ac.cn), Institute of Geographic Sciences and Natural Resources Research, Chinese Academy of Sciences. 11A, Datun Road, Chaoyang District, Beijing 100101, China.

Abstract. Digital soil mapping of soil particle-size fractions (PSFs) using log-ratio methods ~~has been~~is a widely used technique. As a hybrid interpolator, regression kriging (RK) is an alternative way to improve prediction accuracy. However, there is still a lack of systematic ~~comparison~~comparisons and ~~recommendation~~recommendations when RK is applied for compositional data, and ~~whether~~it is not known if the performance based on different balances of isometric log-ratio (ILR) transformation is robust. Here, we systematically compared the generalized linear model (GLM), random forest (RF), and their hybrid pattern (RK) using different balances of ILR transformed data ~~of~~for soil PSFs, with 29 environmental covariables (ECs) for the prediction of soil PSFs ~~on~~in the upper reaches of the Heihe River Basin. The results showed that RF ~~had better performance~~performed best, with more accurate predictions, but GLM ~~had~~produced a more unbiased prediction. For the hybrid interpolators, RK was recommended because it widened the data ranges of the prediction results, and modified the bias and accuracy for most models, especially for RF. ~~The~~ However, there was a drawback~~, however, existed~~ due to the data distributions and model algorithms. Moreover, prediction maps generated from RK ~~demonstrated~~revealed more details of the soil sampling points. For ~~the~~ three components, sequential binary ~~partitions~~partition (SBP) based ILR transformed data ~~made~~produced different distributions, and it is not recommended to use the most abundant component of ~~compositions~~ compositional data as the first component of ~~permutations.~~a permutation. This study ~~can provide~~provides a reference for the spatial simulation of soil PSFs combined with ~~environmental covariables~~ECs and transformed data at ~~a~~the regional scale.

~~**Keywords:** soil particle-size fractions; regression kriging; compositional data; isometric log-ratio; generalized linear model; random forest~~

1 Introduction

Recently, spatial interpolation of soil particle-size fractions (PSFs) has become a focus of ~~researchers in~~ soil science researchers. More ~~accurate~~accurately predicted soil PSFs could contribute to a better understanding of hydrological, physical, and environmental processes (Delbari et al., 2011; Ließ et al., 2012; McBratney et al., 2002).

The ~~characteristic~~characteristics of compositional data makes soil PSFs ~~were~~ more impressive than other soil properties.

Soil PSFs are usually ~~express~~expressed as three components of discrete data – sand, silt, and clay, and carry only relevant percentage information. Soil texture is classified as soil PSFs, which can ~~demonstrate~~be demonstrated on ~~the~~a ternary diagram. ~~This~~The closure system of ~~the~~a ternary diagram is not Euclidean space~~. Instead, it~~, but is rather Aitchison space (~~so-called~~i.e., the simplex) (Aitchison, 1986). Due to ~~the~~ “spurious correlations” (Pawlowsky-Glahn, 1984), traditional statistical methods based on ~~the~~ Euclidean geometry may ~~make~~generate mistakes when dealing directly with soil ~~PSFs~~PSF data ~~directly~~ (Filzmoser et al., 2009). The ~~requirements of~~requirement for constant sum, nonnegative, unbiased ~~are~~values is the key to ~~its~~ spatial interpolation (Walvoort and de Gruijter, 2001). Data transformation is crucial ~~importance~~ for the transformation of compositional data ~~to transform it~~ from the simplex to the real space. Log ratio transformations play a significant role in compositional data analysis, including the additive log-ratio (ALR), centered log-ratio (CLR) (Aitchison, 1986), and isometric log-ratio (ILR) (Egozcue et al., 2003).

~~Currently, though~~Although these three log-ratio methods have been widely applied to transform soil ~~PSFs~~PSF data, different study area scales and ~~what~~ model ~~use~~selection should ~~consider~~be considered when modeling. For local~~-~~ scale study areas, geostatistical models, i.e., ordinary kriging (OK) and compositional kriging, combined with log-ratio transformed data, ~~can meet the requirements~~are sufficient to map spatial patterns virtually, as shown in our previous study (Wang and Shi, 2017). As another perspective, functional compositions combined with the kriging method can also be applied ~~for~~to produce soil particle size curves (~~PSC~~PSCs) (Menafoglio et al., 2014), ~~which can develop fully the richness~~providing an abundance of information. ~~It used~~This involves the use of complete and continuous information rather than discrete information, and soil PSFs can be extracted from the predicted soil PSCs (Menafoglio et al., 2016a). Log-ratio transformations can also ~~combine~~be combined with functional-compositional data for the stochastic simulation of PSCs (Menafoglio et al., 2016b, Talska et al., 2018). For middle~~-~~ scale study areas, outliers may lead to the overestimation of the variogram ~~and make~~, resulting in prediction errors (Lark, 2000). Therefore, the spatial interpolation should take robust variogram estimators into account to improve model performance (Lark, 2003). ~~The~~A previous study ~~has already~~ proved that applying robust variogram estimators in log-ratio co-kriging ~~had significant improvement in~~significantly improved mapping performance (Wang and Shi, 2018). For ~~the~~ large~~-~~scale study ~~area~~areas, geostatistical models are limited by the number of soil sampling points and increased spatial variability. ~~More and more~~An increasing number of studies have concentrated on mapping soil PSFs using different machine learning models, statistical models, and geostatistical models combined with ancillary data (~~so-called~~i.e., environmental ~~covariates, EC~~covariables, ECs) on a broad basin scale (Zhang et al., 2020), national scale (Akpa et al., 2014~~)~~), and global level (Hengl et al., 2017) using log-ratio transformed data.

Among these EC-combined models, linear, machine-learning, geostatistical models, and high accuracy surface modeling (Yue et al., 2020) have been commonly used in middle~~-scale~~ or large-scale studies. Linear models, such as the generalized linear model (GLM) and multiple linear regression (MLR) have been used in soil ~~PSFs prediction~~PSF predictions because of their flexibility and interpretability (Lane, 2002; Buchanan et al., 2012). Many ~~of~~ machine-learning models ~~were~~have been applied for ~~soil PSFs~~the interpolation of soil PSFs and soil texture classification. For example, tree learners~~—~~, such as the random forest (RF), ~~showed more advantages with abilities~~have been shown to be advantageous due to their ability to handle noisy datasets and ~~generated~~generate more realistic maps (Zhang et al., 2020). ~~Further~~Furthermore, regression kriging (RK) can not only combine ~~environment covariables by~~ECs through its regression ~~part~~function, but it also ~~improve~~improves model accuracy as a hybrid interpolator for some soil properties, such as topsoil thickness and pH (Hengl et al., 2004). However, the scope of the comparison needs to be expanded ~~for~~to further ~~exploring~~explore the accuracy ~~assessment to~~and predict compositional data using linear models, machine-learning models, and ~~besides, these~~other models combining RK (hybrid patterns).

In log-ratio methods, the ILR method ~~performed~~performs better than ALR and CLR in both ~~in~~ theory and in practice (Filzmoser and Hron, 2009; Wang and Shi, 2018; Zhang et al., 2020). The ILR method eliminates model collinearity and preserves advantageous properties such as isometry, scale invariance, and sub-compositional coherence, ~~which is based on~~through its use of orthonormal coordinate systems (~~so-called~~i.e., balances) using a sequential binary partition (SBP) (Egozcue and Pawlowsky-Glahn, 2005). These choices are not unique. In other words, multiple sets of ILR transformed data can ~~generate~~be generated by permutations of components (different SBPs) in the compositional data. The choice of ~~SBPs~~an SBP can be based on prior expert knowledge, using a compositional biplot (Lloyd et al., 2012) or variograms and cross-variograms (Molayemat et al., 2018). It has been proven in statistical science that different results ~~were~~are obtained using different choices of SBP balances, and the option of a specific SBP for data compositions is crucial for the intended interpretation of coordinates (Fiserova and Hron, 2011). However, most ~~researchers in~~ soil science researchers have ignored this point. Martins et al. (2016) reported that ~~the~~ clay ~~was taken~~has been widely used as the denominator in the ALR method because it ~~was~~is typically the most abundant component of compositions. Few studies have compared the different SBP options from the perspective of accurate ~~assessment~~assessments and analyzed whether these differences are due to the general characteristics of specific data sets or log-ratio transformations.

Therefore, based on our previous ~~study~~work, the objectives of this study ~~are~~were to: (i) compare the spatial prediction accuracy of soil PSFs using a ~~generalized linear model (~~GLM~~)~~ and ~~random forest (~~RF~~)~~ combined with ~~environmental covariables~~ECs and ILR transformed data; (ii) determine whether hybrid interpolators (GLMRK and RFRK) can improve the interpolation performance of a GLM and RF; and (iii) explore the distributions of different transformed data and the variation law of precision based on different choices of SBP balances of ILR.

2 Methods and materials

2.1 Study area

The study area ~~is~~was the upper reaches of the Heihe River ~~basin~~Basin (HRB), which is the ~~birthplace~~source of the Heihe River and the central area of ~~the~~ runoff generation ~~of~~in the HRB. The elevation ~~is~~in this area ranges from 1640 ~~m~~ to 5573 m (Fig. 1), and the climate is damp and cold, being dominated by the Qilian Mountains. The mean annual rainfall ~~of this~~in the study area is 350 mm, and the mean annual temperature is lower than 4~~-~~°C. Meadow and steppe ~~dominate~~are the dominant vegetation types. Grassland ~~was~~is the primary ~~type of~~ land use. The main soil classes are frigid calcic soil in the southwest of ~~this~~the study area, with cold desert soil ~~dominates~~dominating the southeast, ~~and~~while Castanozems and Sierozems ~~mainly distribute~~are distributed in the north of the study area.

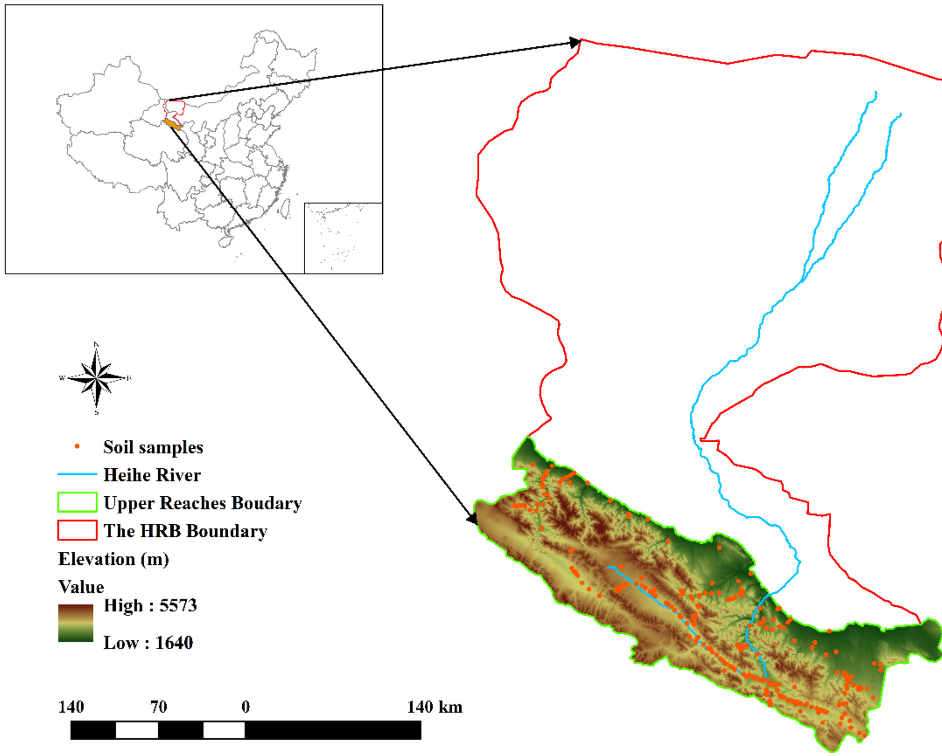

Figure. 1. The location, elevation, and soil samples on the upper reaches of the Heihe River Basin.

2.2 Data collection and analysis

2.2.1 Soil PSF data

A total of 262 soil samples ~~based on a purposive sampling strategy~~ were collected in the upper reaches of the HRB based on a purposive sampling strategy and were used to characterize the spatial variability of soil PSFs at the regional-scale ~~study area~~ (Fig. 1). The variability of soil formation factors, such as ~~the~~ elevation, soil ~~classes~~type, vegetation ~~classes~~class, and geomorphology ~~classes~~ of the upper reaches of the HRB was considered in soil ~~samples~~sample collection. The average of three mixed ~~three~~ topsoil samples (~~approximately~~ approximate depth of 0–20 cm) was obtained to reduce the noise of soil ~~samples~~sample parameters, and ~~the~~a parallel sample was also measured. Subsequently, about 30 g of each soil sample was air-dried, and ~~the~~ chemical and physical analyses were ~~operated after the fieldwork. Collected~~ conducted in the laboratory. Soil PSF information was obtained for the soil samples ~~recorded the information about soil PSFs~~ using a Malvern Panalytical Mastersizer 2000 ~~laser~~, with less than 3% average measurement error.

2.2.2 The selection of ~~environmental covariables~~ECs

There were 29 ~~environmental covariates~~ECs considered in our study, including both continuous and categorical variables~~, which were considered in our study~~ (Table 1). They ~~follow~~followed the principles of the SCORPAN model (McBratney et al., 2003), which~~ form~~ is defined as $S_a = f(S, C, O, R, P, A, N)$. S_a are soil attributes (or classes) as a function of soil properties (S) or other properties~~—~~, i.e., climatic properties (C), organisms and vegetation (O), relief such as topography and landscape attributes (R), parent material (P), an age or time factor (A~~)~~), and spatial position (N). The continuous variables included the morphometry and hydrologic characteristics of topographic properties, climatic and vegetative indices, and soil physical and chemical properties. The categorical variables ~~include~~included geomorphology~~ types~~, land use types, and vegetation ~~types~~classes, which were transformed from vector to raster (1000 m). Due to the intricate patterns of topography in the upper reaches of the HRB, ~~variables~~the variable of topographic properties dominated the ~~environmental covariates.~~ ECs. The System for Automated Geoscientific Analyses geographic information system (SAGA GIS) (Conrad et al., 2015) was applied for a terrain analysis to derive topographic variables using the 30 m ~~DEM~~resolution Advanced Spaceborne Thermal Emission and Reflection Radiometer Global Digital Elevation Model (ASTER GDEM, http://www.gscloud.cn). ~~The~~A collinearity test ~~can remove~~removed the redundant variables, and ~~then these~~the topographic properties were then resampled to 1000 m. More details ~~about environmental covariables can be found~~of the ECs are provided in the Data Availability section.

Table 1. Selected environmental covariates in our study.

Representation	Environment covariables	Abbreviation
Morphometry characteristics	Analytical Hill Shading	AHS
	Aspect	ASPECT
	Closed Depressions	CD
	Convergence Index	CI
	Channel Network Base Level	CNB
	Slope Length and Steepness Factor	LSF
	Multi-resolution Ridge Top Flatness Index (Gallant and Dowling, 2003)	MRRTF
	Multi-resolution Valley Bottom Flatness Index (Gallant and Dowling, 2003)	MRVBF
	Mid-slope Position	MSP
	Plan Curvature	PLC
	Profile Curvature	PRC
	Slope Height	SH
	Slope Length (D. Moore et al., 1993)	SL
	Tangential Curvature (Florinsky, 1998)	TC
Hydrologic characteristics	Catchment Area	CA
	Surface Area	SA

	Stream Power Index	SPI
	Topographic Wetness Index (Beven and Kirkby, 1979)	TWI
	Vertical Distance to Channel Network	VDCN
Climatic and vegetative indices	Average Annual Precipitation	RAIN
	Average Annual Temperature	TEM
	Normalized Differential Vegetation Index	NDVI
Soil physical and chemical properties	Field Water Holding Capacity (Yi et al., 2015; Song et al., 2016; Yang et al., 2016)	FWHC
	Soil Depth (Yi et al., 2015; Song et al., 2016; Yang et al., 2016)	PDEPTH
	Saturated Hydraulic Conductivity (Yi et al., 2015; Song et al., 2016; Yang et al., 2016)	SHC
	Soil Organic Carbon	SOC
Categorical maps	Geomorphology	GEOT
	Land Use	LU
	Vegetation Classes	VEGET

2.3 Isometric log-ratio transformation and ~~sequential binary partition~~SBP

An orthonormal basis of the ILR was chosen to isometrically project the compositions from S^D (the simplex for the Aitchison geometry) to R^{D-1} (real space for the Euclidean geometry~~) isometrically.~~). The choice of a specific orthonormal basis for use on S^D can be explained by the SBP ~~with their~~for the groups of compositions (Egozcue and Pawlowsky-Glahn, 2005). The ~~equation for the~~ choice of the construction of coordinates (~~so-called~~i.e., balances) between groups of compositions ~~is~~was calculated as follows:

$$z_k = \sqrt{\frac{r_k s_k}{r_k + s_k}} ln(\frac{(x_{i_1} x_{i_2} \dots x_{i_{r_k}})^{1/r_k}}{(x_{j_1} x_{j_2} \dots x_{j_{s_k}})^{1/s_k}}),\ k = 1, \dots, D-1, \quad (1)$$

where z_k refers to the balance between two groups~~,~~; $i_1, i_2, \dots, i_{r_k}$ is the r_k ~~parts~~part of one group~~,~~; and $j_1, j_2, \dots, j_{r_k}$ is the s_k ~~parts~~part of the other group. Therefore, in a stepwise manner, the balances contain ~~stepwise~~ all the relevant information of the compositions in two groups. ~~It~~This can also ~~can~~ be explained in a tabular form~~— for~~. For soil ~~PSFs~~PSF data (D = 3), all three choices of the balance of SBPs are shown in Table 2. The first component of the ILR ~~contains~~contained all the information on soil PSFs, and the main difference ~~of~~in the choice of balances for soil PSFs was the order of the three parts, i.e., the first order of the soil PSF component was used as the numerator of the first ILR equation. In our study, three SBP balances~~ of SBP —~~, SBP1, SBP2, and SBP3, were transformed from the original soil PSF data, and the orders of soil PSF data were $(sand, silt, clay)$, $(silt, clay, sand)$, and $(clay, sand, silt)$, respectively. The transformation ~~equation~~equations for the ILR can be derived from Eq. (1), ~~which was~~and were defined as ~~Eq~~Eqs. (2) and ~~Eq.~~ (3). The inverse equations for ILR were defined as ~~Eq~~Eqs. (4), (5), (6). The ILR transformation and its inverse ~~are available in~~were conducted using the R package "compositions" (K. Gerald van den Boogaart and Raimon Tolosana, 2014).

$$\mathbf{z} = (z_1, \dots z_{D-1}) = ILR(\mathbf{x}), \text{ and for } i = 1, \dots, D-1 \text{ and component } x_i, \tag{2}$$

$$z_i = \sqrt{\frac{D-i}{D-i+1}} \, ln \frac{x_i}{\sqrt[D-i]{\prod_{j=i+1}^{D} x_j}}. \tag{3}$$

$$Y(x_j) = \sum_{j=1}^{D} \frac{ILR(x_j)}{\sqrt{j \times (j+1)}} - \sqrt{\frac{j-1}{j}} \times ILR(x_j), \tag{4}$$

$$ILR(x_0) = ILR(x_D) = 0, \tag{5}$$

$$\overline{ILR}(x_j) = \frac{exp(Y(x_j))}{\sum_{j=1}^{D} exp(Y(x_j))}. \tag{6}$$

Table 2 All choices of SBPs for soil PSF data (D = 3), the orders of soil PSFs data are $(sand, silt, clay)$, $(silt, clay, sand)$ and $(clay, sand, silt)$ for SBP1, SBP2 and SBP3.

Groups	Step	Sand	Silt	Clay	r	s	Balance
SBP1	1	+	-	-	1	2	Step1: $z_1 = \sqrt{\frac{2}{3}} \, ln \frac{sand}{\sqrt{silt \times clay}}$
	2	0	+	-	1	1	Step2: $z_2 = \sqrt{\frac{1}{2}} \, ln \frac{silt}{clay}$
SBP2	1	-	+	-	1	2	Step1: $z_1 = \sqrt{\frac{2}{3}} \, ln \frac{silt}{\sqrt{clay \times sand}}$
	2	-	0	+	1	1	Step2: $z_2 = \sqrt{\frac{1}{2}} \, ln \frac{clay}{sand}$
SBP3	1	-	-	+	1	2	Step1: $z_1 = \sqrt{\frac{2}{3}} \, ln \frac{clay}{\sqrt{sand \times silt}}$
	2	+	-	0	1	1	Step2: $z_2 = \sqrt{\frac{1}{2}} \, ln \frac{sand}{silt}$

2.4 Linear model, machine-learning model, and hybrid patterns

2.4.1 Generalized linear model

The ~~generalized linear model (~~GLM~~)~~ is an extended version of the linear model, which contains response variables, with non-normal distributions (Nelder and Wedderburn, 1972). The link function is embedded into the GLM to ensure the classical linear model assumptions. The scaled dependent variables and the independent variables can be connected using a link function for the additive combination of model effects, the choice of link function depends on the distribution of response variables (Venables and Dichmont, 2004). A Gaussian distribution with an identity link function was applied in our study, which

~~gives~~produced consequences equivalent to that of ~~multiple linear regression~~MLR (Nickel et al., 2014). However, categorical variables can be directly trained in the GLM without setting dummy variables. The Akaike's information criterion (AIC) was applied to choose the best predictors and remove model multicollinearity using a backward stepwise algorithm.

2.4.2 Random forest

~~Random forest (~~The RF~~)~~ is a non-parametric technique, which combines the bagging method with a selection of random variables as an extended version of a regression ~~trees~~tree (RT) (Breiman, 1996, 2001). It can improve model prediction accuracy by producing and aggregating multiple tree models. The principle of the RF is to merge a group of "weak trees" together to generate a "powerful forest." The bootstrap sampling method ~~is~~was applied for each tree, and each predictor was selected randomly from all model predictors. The "out of bag" (OOB) data were applied to produce reliable estimates in an internal validation using a random subset independent of the training tree data. ~~There are three~~Three parameters ~~need~~needed to be tuned: ~~the~~ number of trees ($ntree$~~) and~~); minimum size of terminal nodes ($nodesize$), and~~ the~~ number of variables randomly sampled as predictors for each tree ($mtry$) (Liaw and Wiener, 2001). The standard value of the $mtry$ parameter ~~for $mtry$ is~~was one-third of the total number of predictors, while $ntree$ and $nodesize$ ~~is~~were 500 and 5, respectively. For regression, the mean square errors (MSEs) of predictions were estimated to train the trees. The variable importance of the RF ~~is~~was produced from the OOB data using the "importance" function. ~~The~~One of the benefits of ~~RFs are~~the RF is that the ensembles of trees are used without pruning to ensure that the most significant amount of variance can be expressed. Moreover, the RF can reduce model overfitting~~,~~ and normalization is unnecessary due to the ~~insensitive~~ effects on the value range~~.~~ being insensitive. The GLM and RF algorithms ~~of GLM and RF~~ and the ~~parameters~~parameter adjustment of the RF were ~~available~~conducted in the R package "caret" (Max Kuhn, 2018).

2.4.3 Regression kriging

Regression kriging ~~(RK)~~ is a hybrid interpolation technique that combines regression models (e.g., GLM and RF) with ~~ordinary kriging (~~the OK~~)~~ of the residuals of regression models (Odeh et al., 1995). Mathematically, the RK method corresponds to two interpolators~~—~~, the regression part and the kriging part, which are operated separately (Goovaerts, 1999). ~~A~~One limitation of using only the regression part is that ~~they are~~it is usually only useful within the range of values of the training sets (Hengl et al., 2015). The principle of the RK method is that the regression model explains a deterministic component of spatial variability, and the interpolation of regression residuals generated from OK is used to describe the spatial variability (Bishop and McBratney, 2001; Hengl et al., 2004). ~~Residuals~~The residuals are used to create a variogram (e.g., Gaussian, ~~Spherical~~spherical, or ~~Exponential~~exponential) for ~~model~~models based on the MSE from the results of a cross-validation. ~~Firstly~~First, the regression part in our study (GLM or RF) was used to predict soil PSFs~~; the~~. The residual from the fitted model was then calculated by subtracting the regression part from the observations. Subsequently,~~ the~~ OK was applied for the whole study area to interpolate the residuals. Finally, the regression prediction and the predicted residuals at the same location were summed.

The variograms of the RK method were generated automatically ~~by~~ using the "autofitVariogram" function in the R package "automap" (Hiemstra et al., 2009).

2.5 Prediction method system and validation

The method system of spatial interpolation models for soil PSFs ~~was revealed~~is presented in Table 3. We systematically compared 12 models~~—~~: four interpolators, including GLM and RF ~~combined~~ with or without RK, and three SBPs of the ILR transformation method. For the validation of model performance, the independent data set validation was used to evaluate the prediction bias and accuracy of the models. The sub-training sets (70~~-~~%) and the sub-testing sets (30~~-~~%) were randomly ~~divided~~selected from data independently, and this process was repeated 30 times.

Table 3. The method system of spatial interpolation models of soil PSFs.

Models	GLM	GLMRK	RF	RFRK
ILR_SBP1	GLM_SBP1	GLMRK_SBP1	RF_SBP1	RFRK_SBP1
ILR_SBP2	GLM_SBP2	GLMRK_SBP2	RF_SBP2	RFRK_SBP2
ILR_SBP3	GLM_SBP3	GLMRK_SBP3	RF_SBP3	RFRK_SBP3

The mean error (ME), the root mean square error (RMSE), and Aitchison distance (AD) were used to evaluate and compare the prediction performance of models. The ME and RMSE measure prediction bias and accuracy, respectively (Odeh et al., 1995). The AD is an overall indicator of compositional analysis, which describes the distance between two data compositions. Generally, in an accurate, unbiased model ~~will have~~ all three ~~symbols~~values will be close to 0. The ~~equations for~~ ME, RMSE, and AD ~~are defined~~were calculated as follows:

$$ME = \frac{1}{n}\sum_{i=1}^{n}(M_i - P_i), \tag{7}$$

$$RMSE = \sqrt{\frac{1}{n}\sum_{i=1}^{n}(M_i - P_i)^2}, \tag{8}$$

$$AD = \left[\sum_{i=1}^{D}(log\frac{M_i}{G(\boldsymbol{M})} - log\frac{P_i}{G(\boldsymbol{P})})^2\right]^{0.5}, \tag{9}$$

where M_i and P_i are the measured ~~value~~ and predicted ~~value~~values at the ith position, respectively; n refers to the number of soil samples; D is the number of dimensions of data compositions; and $G(\boldsymbol{M})$ and $G(\boldsymbol{P})$ ~~denotes~~denote the geometric mean with the form $\mathrm{G}(\mathbf{x}) = \cancel{(x_1, \ldots, x_D)^{1/D}\ \text{of}}(x_1, \ldots, x_D)^{1/D}$ of the measured and predicted values, respectively.

2.6 Statistical analysis

~~An~~The interpretation of the balances of ILR is based on a decomposition of the covariance (COV) structure (Fiserova and Hron, 2011~~), we~~). We calculated the variance (VAR), ~~the covariance (~~COV~~)~~, and the corresponding correlation coefficient (CC) of ILR transformed data based on different SBP balances~~ of SBP~~. The equations for calculating VAR, COV, and CC ~~are~~

~~defined~~were derived from Eq. (1) as follows~~, which can derive from Eq (1):~~:

$$VAR(z)=\frac{1}{r+s}\sum_{p=1}^{r}\sum_{q=1}^{s}var(\ln\frac{x_{i_p}}{x_{j_q}})-\frac{s}{2r(r+s)}\sum_{p=1}^{r}\sum_{q=1}^{r}var(\ln\frac{x_{i_p}}{x_{i_q}})-\frac{r}{2s(r+s)}\sum_{p=1}^{s}\sum_{q=1}^{s}var(\ln\frac{x_{j_p}}{x_{j_q}})-\frac{r}{2s(r+s)}\sum_{p=1}^{s}\sum_{q=1}^{s}var(\ln\frac{x_{j_p}}{x_{j_q}}) \quad (10)$$

$$COV(z_1,z_2)=\frac{C}{2r_1s_2}\sum_{p=1}^{r_1}\sum_{q=1}^{s_2}var(\ln\frac{x_{i_p^1}}{x_{j_q^2}})+\frac{C}{2r_2s_1}\sum_{p=1}^{r_2}\sum_{q=1}^{s_1}var(\ln\frac{x_{i_p^2}}{x_{j_q^1}})-\frac{C}{2r_1r_2}\sum_{p=1}^{r_1}\sum_{q=1}^{r_2}var(\ln\frac{x_{i_p^1}}{x_{i_q^2}})-\frac{C}{2s_1s_2}\sum_{p=1}^{s_1}\sum_{q=1}^{s_2}var(\ln\frac{x_{j_p^1}}{x_{j_q^2}}), \quad (11)$$

$$CC=\frac{COV(z_1,z_2)}{\sqrt{var(z_1)\cdot var(z_2)}} \quad (12)$$

For soil ~~PSFs~~PSF data, ~~Eq~~Eqs. (10), (11~~)~~), and (12) can be simplified to three dimensions~~; the~~. The relationship between the ratios of soil PSF components and the dominant roles of ILR transformed data ~~are demonstrated~~were indicated from the covariance structure. All the statistical analyses, such as the descriptive statistics of soil ~~PSFs~~PSF data, calculation and evaluation of indicators, and the spatial operation of prediction maps, were performed ~~on~~using the R statistical program (R Development Core Team, 2019).

3 Results

3.1 Exploratory data analysis

3.1.1 Descriptive statistics of soil ~~PSFs~~PSF data

~~For~~From the descriptive statistics of the original (raw) and ILR transformed data, the silt fraction ~~dominant~~ dominated the soil PSFs~~ with~~, accounting for a more substantial ~~component~~amount than ~~those of~~the sand and clay fractions. The distributions of the sand and clay fractions were similar (Fig. 2a). The ILR transformed data based on the three SBP balances ~~of SBP were~~ revealed different distributions (Figs. 2b, 2c, and 2d). For example, two ILR components ~~of ILR~~ (ILR1~~,~~ and ILR2) for SBP1 had a symmetric distribution around zero ~~value~~ at the *x*-axis (Fig. 2b). In comparison, the distribution of data generated from SBP2 or SBP3 had ~~to mirror-symmetric deliveries~~a mirrored symmetry, with a left-skewed ILR1 of SBP2 and right-skewed ILR2 of SBP3 (Figs. 2c and 2d). The comparison of means and medians demonstrated that the back-transformed means of three sets of ILR transformed data were the same, and the mean ILR of sand ~~of ILR~~ was closer to the median compared with the original soil PSF ~~original~~ data. In contrast, the ~~cases of component~~opposite patterns were apparent for the silt and clay ~~were the opposite~~ components (Fig. 2e).

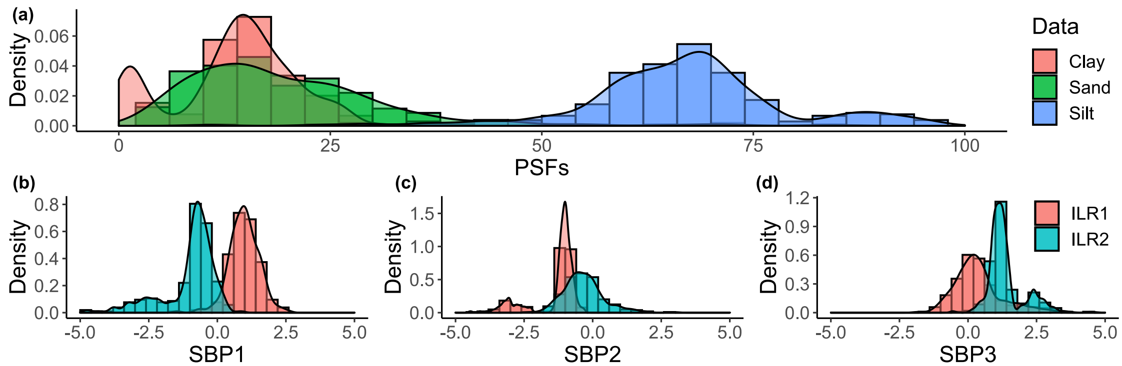

(e)

Center	Sand	Silt	Clay	Sand_ILR	Silt_ILR	Clay_ILR
Mean	19.61	66.80	13.59	18.07	71.48	10.45
Median	17.03	67.44	14.53	—	—	—

Figure. 2. Descriptive statistics of original soil PSF data and ILR transformed data using different balances of SBP**.** Not that means of Sand_ILR, Silt_ILR, and Clay_ILR from different SBPs of ILR were back-transformed to the real space.

3.1.2 Covariance structure of ILR transformed data with different balances

The covariance analysis of the transformed data of soil PSFs ~~data~~ based on the different SBPs showed that the variance VarILR_1 of SBP3 was ~~maximum~~the largest, followed by the ~~values of~~ VarILR_1 of SBP1 and SBP2 (Table 4). The variance of the second component of ILR (VarILR_2) ~~was~~followed the opposite pattern to ~~the rule~~that of VarILR_1. The ~~covariance (~~COV~~)~~ and ~~the~~ corresponding ~~correlation coefficient (~~CC~~)~~ followed the same pattern ~~–~~of SBP1 > SBP3 > SBP2. From these values, the ~~relationship of~~relationships among soil ~~PSFs~~PSF components or ratios were revealed~~, as we have known, the~~. The first ILR equation ~~of ILR~~ (z_1 in Table 2) contained all the soil PSF information~~ of soil PSFs, and~~, while the second one (z_2 in Table 2) included only two components~~; the~~. The VarILR_1 information ~~of VarILR_1,~~was therefore~~, was~~ more abundant. Six values of VarILR_1 and VarILR_2 were not 0 (or not nearly 0), indicating that there was no constant (or almost ~~the~~ constant) value in any two ratios of soil PSF components. The COV value of ~~COV of~~ SBP3 was close to 0, ~~showing~~indicating that the proportions of *clay/sand* and *clay/silt* were approximately the same. The same results were generated from the corresponding ~~correlation coefficient (CC).~~CC.

Table 4 Covariance analysis of soil PSF data based on different SBPs. VarILR_1 and VarILR_2 denote the variance of the first and the second component of ILR, respectively. COV refers to the covariance of ILR1 and ILR2. CC is the correlation coefficient.

Balances	VarILR_1	VarILR_2	COV	CC
SBP1	0.53	0.71	0.32	0.52

SBP2	0.39	0.86	-0.24	-0.41
SBP3	0.94	0.30	-0.09	-0.16

The distribution of soil ~~PSFs~~PSF sampling data in ~~the~~a ternary diagram (the United States Department of Agriculture (USDA) texture triangle) showed that the main texture class was silt loam (Fig. 3a). The biplot of soil samples demonstrated that the rays of the three components, i.e., sand, silt, and clay, were reasonably well clustered at about 120~~-~~° in the three groups (Fig. 3b).

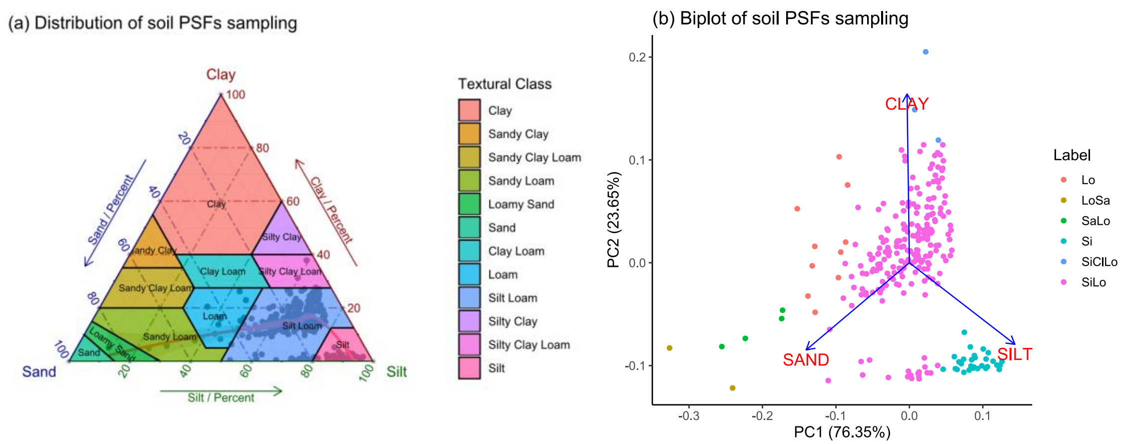

Figure. 3. The distribution in the USDA triangle (a) and biplot graph (b) of soil PSFs sampling. The red, smooth curve of these soil samples in the USDA triangle was fitted by loess function in R.

3.2 Accuracy comparison of different models using ILR data

The first three rows of the boxplots ~~(~~in Figs. ~~4 a~~4a, 4b, and 4c~~) demonstrated~~ indicate the bias of the different models according to their ME values. The ~~MEs~~ME of sand ~~were~~was closest to 0, followed by the MEs of clay and silt. The GLM was more unbiased than the RF, with lower ME values. After ~~combing~~combining with RK, ~~the~~there was an improvement ~~was revealed~~in the ME for ~~MEs in~~ most GLM and RF models (Figs. 4a, 4b, and 4c). For the accuracy assessment, ~~RMSEs~~the RMSE of silt was higher than for the other two components. The GLMRK did not perform as well as ~~expect for RMSEs, which~~ expected in terms of the RMSE, with only ~~improved RMSEs of~~ the sand component having an improved RMSE (Fig. 4d). However, the RFRK ~~had~~performed better ~~performance when compared with~~than the GLMRK and improved the RMSE of most ~~RMSEs of~~ parts compared with the RF, except for the RFRK_SBP1 of sand. ~~Overall~~As an overall indicator of soil PSFs, the AD~~,~~ showed that the RF (or RFRK) performed better than the GLM (or GLMRK) in terms of both average RMSE values and uncertainties (Fig. 4g). Moreover, the RFRK improved the AD values for the SBP2 and SBP3 methods. For the uncertainty assessment, the RF generated ~~lower~~fewer difficulties than the GLM, and the models combined with RK further reduced the uncertainties for most GLM and RF models. ~~For three balances of SBP methods,~~ The model performances were different~~.~~ for the three SBP balances. To better evaluate model performance using the different SBP balances, we graded each box from 1 to 3, and the final results ~~were~~are shown in the Supplementary Material ~~table~~(Table S1.1~~. It~~). The results demonstrated that SBP1 performed best, with the lowest ME value ~~among~~of all models. For the accuracy comparison~~, the pattern is not~~ there was no apparent pattern, but ~~it can~~accuracy could be considered hierarchically. For the GLM, SBP1 ~~had~~performed better ~~performance~~ than the other two ~~SBPs~~SBP methods, which also performed well when RK was added (GLMRK). For RF, SBP1 produced the best result. However, the introduction of RK ~~made~~resulted in SBP3 ~~performed~~performing best among the three methods. ~~Further, the~~The RMSEs generated from RFRK using SBP3 data had the best accuracy among all the models in our study.

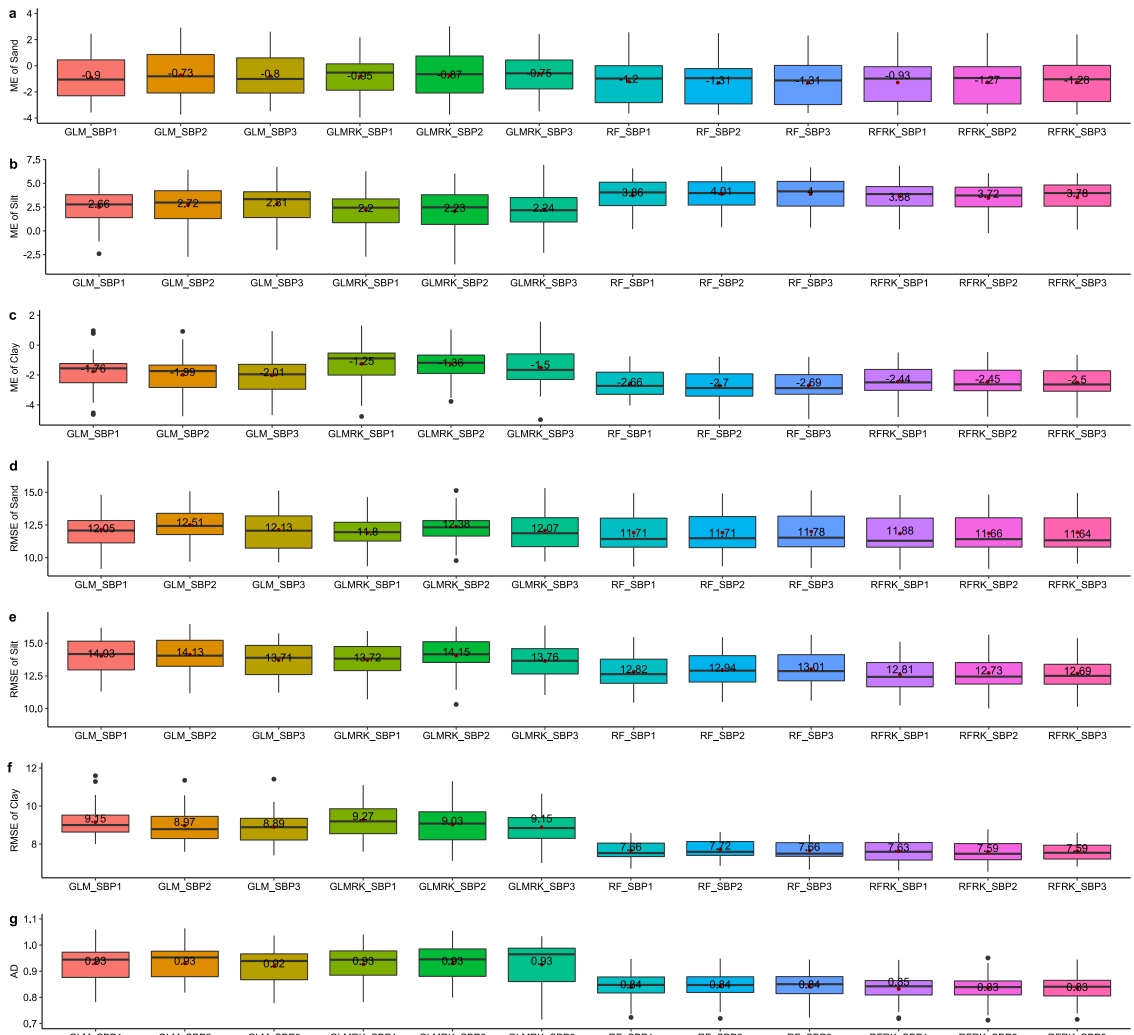

Figure. 4. Accuracy comparison of GLM, RF, and their RK patterns using different ILR balances data. The mean values of different model indicators were calculated in their boxes.

3.3 Spatial prediction maps of soil PSFs generated from the different models

Prediction maps of soil PSFs made from the different models ~~were revealed~~are shown in Figs. 5, 6, and 7. For the components of soil PSFs, the maps of the three group maps followed a similar rule. The GLM and GLMRK ~~showed~~produced more extensive ranges of predicted ~~value~~values, and their maps were more relevant to the real environment. However, the RF and RFRK predicted a relatively narrow ~~and~~range of low values ~~of~~for these components, revealing a smoother distribution than ~~GLMs. Moreover, RK~~ that generated by the GLM and GLMRK. Unlike the regression methods~~ demonstrated hot spots~~, the RF and RFRK methods produced hot and cold spots on the prediction maps ~~compared with only regression parts;~~and more details of the soil sampling points were apparent (Fig. S2.1) ~~were shown~~.

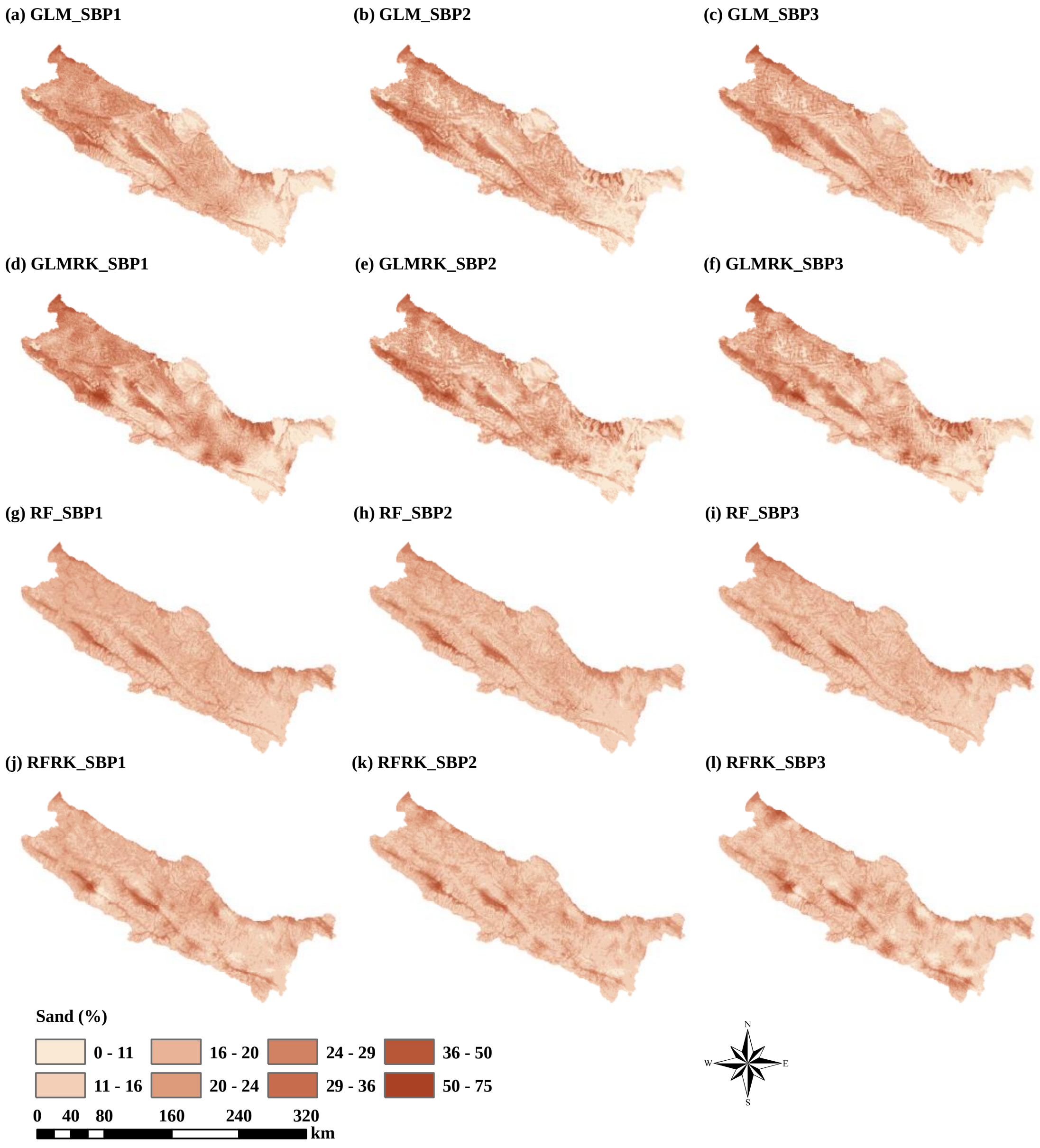

Figure. 5. Spatial prediction maps of the sand component of the upper reaches of the Heihe River Basin.

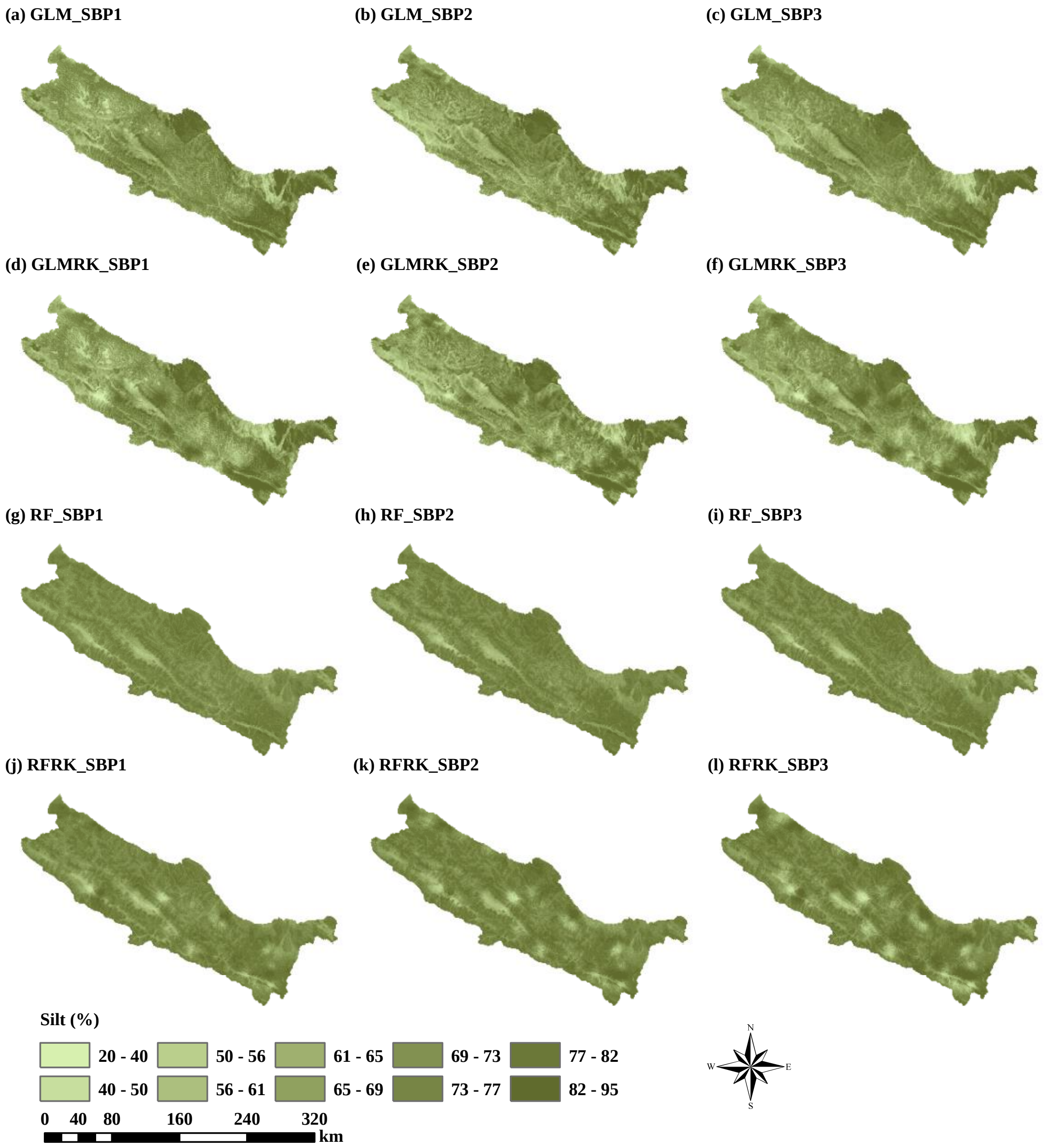

Figure. 6. Spatial prediction maps of the silt component of the upper reaches of the Heihe River Basin.

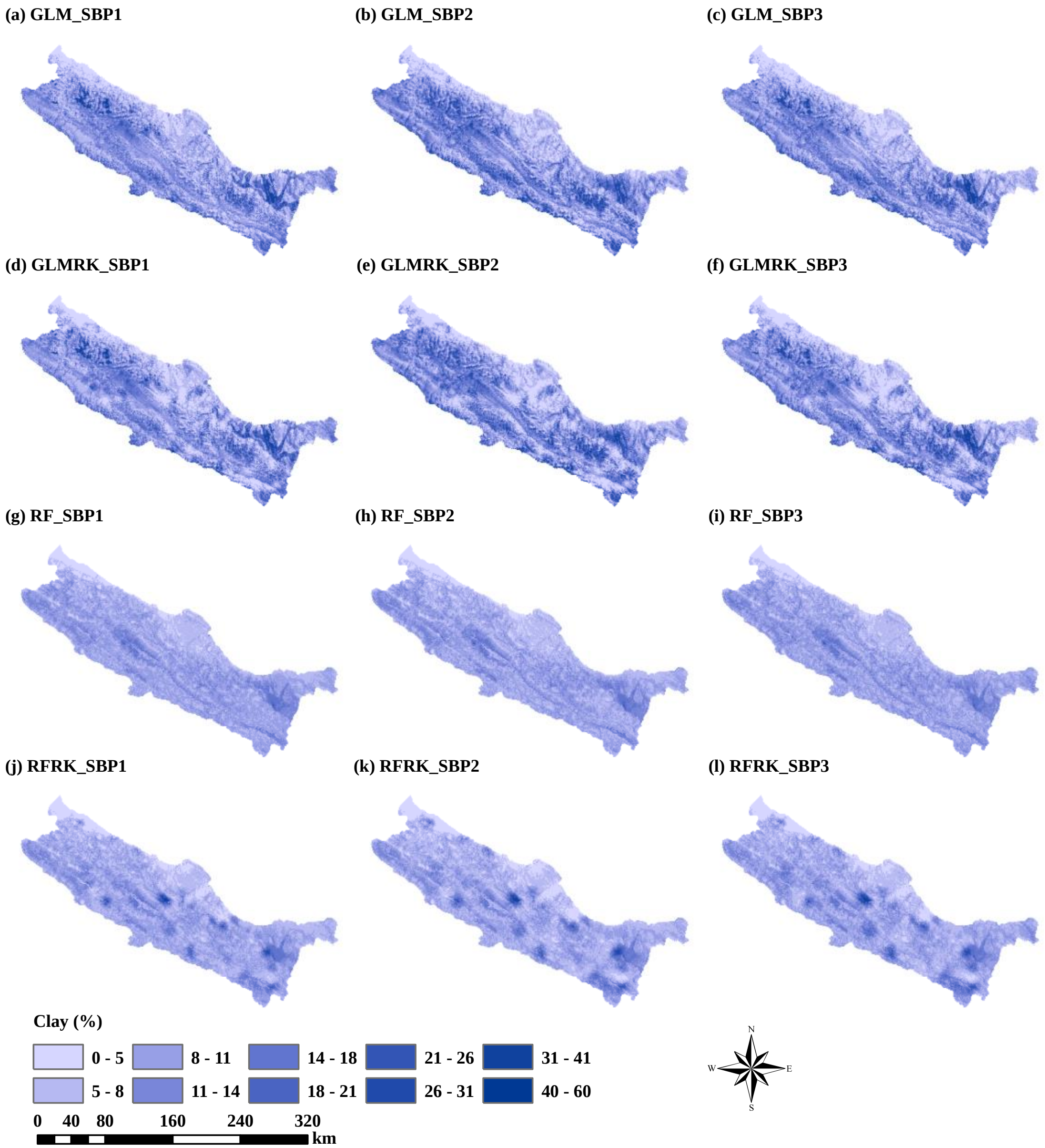

Figure. 7. Spatial prediction maps of the clay component of the upper reaches of the Heihe River Basin.

3.4 Spatial distribution of soil texture classes in the USDA triangles

The predicted soil textures ~~plotted in Fig. 8 in~~based on the USDA texture triangles (Fig. 8) showed that most ~~predicted soil textures~~predictions fell within the ~~ranges~~range of observed soil textures (Fig. 3a), and silt loam was the dominant ~~in the~~ soil texture ~~types for~~in all ~~the~~ cases. The GLM produced a more discrete distribution than the RF, and the RK method expanded the effect of dispersion. ~~For~~In the trends of the predicted samples, the silt components predicted from all models were ~~over-~~

~~estimated~~overestimated. The pattern fitting curves indicated that the prediction results were closer to the bottom right of the USDA soil texture triangle than the soil ~~PSFs~~PSF observations. ~~Curves of~~The GLMRK and RFRK curves were longer than the GLM and RF~~, showing~~ curves, with a more extensive ~~ranges~~range of ~~value~~values in the ternary diagram. Compared with the GLMRK, the RFRK produced a more upward extension (~~Fig~~Figs. 8j, k, l). It was clear that the clay fraction was ~~over-estimated,~~overestimated and the sand fraction was ~~under-estimated~~underestimated.

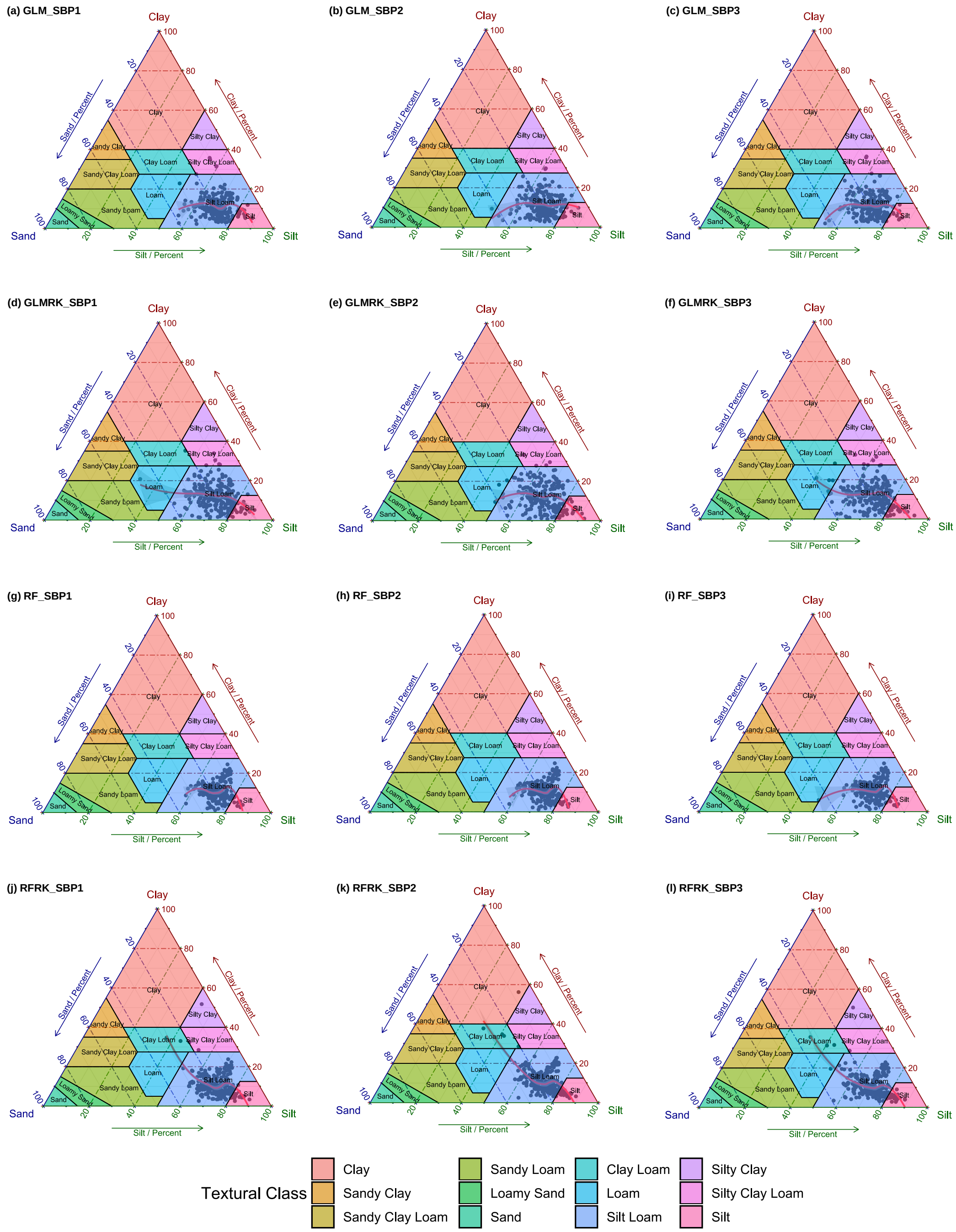

Figure. 8. Predicted 262 soil samples based on leave-one-out method in USDA texture triangles using (a) GLM_SBP1, (b) GLM_SBP2, (c) GLM_SBP3, (d) GLMRK_SBP1, (e) GLMRK_SBP2, (f) GLMRK_SBP3, (g) RF_SBP1, (h) RF_SBP2, (i) RF_SBP3, (j) RFRK_SBP1, (k) RFRK_SBP2, (l) RFRK_SBP3. Red fitting lines in triangles showed the trends.

4 Discussion

4.1 Comparison of the GLM, RF, and their hybrid interpolators using ILR data

The range of applicability of this study is limited to independent modelling. However, the study demonstrated the correlation of the raw data (sand, silt, and clay), and has confirmed that the currently used prediction models are suitable. For the assessment of independent validation, the RF revealed more accurate results, but with more bias than the GLM. The RK method improved the bias performance ~~of the bias~~ for most models and the accuracy of the RF. Odeh et al. (1995) ~~have~~ indicated that RK was superior to the linear models, such as ~~the multiple linear regression (~~MLR~~)~~,, which ~~can be~~was reflected in the prediction ~~of~~results for sand in our study. Scarpone et al. (2016) reported that as a hybrid interpolator, the RFRK outperformed the RF when ~~dealing with~~making soil thickness ~~prediction~~predictions. We proved that RK was also ~~available~~suitable for compositional data ~~to improve~~and improved model performance when using an ILR transformation in the RF. In summary, the GLM and RF had ~~their~~both advantages and disadvantages when considering the trade-off between bias and accuracy. The difficulty with the use of the GLM is the need for a back-transformation~~; it needs~~. There is a need to present results on the original untransformed scale after ~~analyzing~~conducting the analysis on a transformed level, which may produce ~~the unfortunate result between them~~spurious results (Lane, 2002). In our study, we compared the means of ILR transformed data and the original data. We proved the feasibility of the ILR transformation method, especially for meeting the requirements of compositional data. ~~Still~~However, the accuracy of the GLM still needs to be improved~~; this~~, which may be because the transformed data did not follow a normal distribution. In addition, although the RF had ~~an~~the advantage ~~on~~of prediction accuracy, the limited interpretability of the consequences – a "black box" effect – made it ~~challenging~~difficult to modify the prediction bias because each tree from the model cannot be examined individually (Grimm et al., 2008). The ILR transformation before modeling increased the difficulty of interpretation for not only the predicted values on the ILR~~-~~ scale but also the residuals. Moreover, the back-transformation of the optimal estimate of log-ratio variables does not generate the optimal estimation of ~~compositions~~compositional data (Lark and Bishop, 2007), which ~~also~~ should also be considered. Multivariate methods, such as the multivariate RF, can be combined with a log-ratio transformation and hybrid interpolation, enabling the cross correlations among ILR coordinates to be better interpreted.

4.2 Comparison of three SBP balances ~~of~~in the ILR transformation method

The results of GLM and GLMRK should not depend on the ILR basis being chosen, which has been proved by previous studies on the use of linear models and kriging for compositional data (Pawlowsky-Glahn et al, 2015). However, the GLM model used the "glmStepAIC" algorithm (i.e., a stepwise regression) to select the best combination of environmental covariables for each ILR component. Therefore, the variable inputs were different for these ILR data, and further impact the accuracy assessment and prediction maps.

The comparison of the three SBP balances ~~of SBP~~ showed that ~~most~~the indicators of ME and RMSE performed better when using SBP1 ~~of~~for ILR transformed data~~ performed better~~, which may be interpreted as the distributions of the ILR1 and ILR2 of SBP1 ~~were~~being more symmetric (Fig. 2b). In contrast, the performance of SBP2 was worse than ~~the other two~~ that of SBP1 and SBP3 because the ILR_1 component, including all the soil PSF information~~ of soil PSFs~~, was left-skewed (Fig. 2c). This result was ~~apparent,~~ especially apparent for the GLM and GLMRK, because the ~~normal distribution of~~ data ~~is needed~~ in ~~the~~a linear model needs to be normally distributed (Lane, 2002).

The interpretation of the negligible difference among the three SBP balances ~~of SBP~~ was ~~the~~ presented in a biplot of soil ~~PSFs~~PSF sampling data (Fig. 3b), which revealed a triangular shape. ~~In other words, these can~~This could be interpreted as ~~that~~the three soil PSFs ~~had~~having a mixed pattern, ~~and~~with each component ~~was~~ dominated by the components in one cluster (Tolosana-Delgado et al., 2005). Although the silt component dominated the soil PSFs ~~with the highest content~~ (Fig. 2a), sand and clay also played ~~essential~~important roles ~~of~~in the compositional data~~ as well~~. Therefore, taking either the most abundant component of ~~compositions~~the compositional data as the denominator (Martins et al., 2016) or the first component of the permutations ~~was~~did not provide convincing evidence. ~~In contrast, using~~Using the most abundant component of ~~compositions~~ the compositional data as the primary component of the alterations, i.e., SBP2, ~~demonstrated~~resulted in a relatively poor performance ~~among three~~ compared to the other SBPs~~ data~~. Thus, we ~~recommended~~recommend using other parts that ~~were~~are not the most abundant as the first component of permutations~~ when the biplot diagram was~~, which in this case resulted in a uniform distribution on the biplot diagram, with a cluster at about 120~~-~~° (Fig. 3b). Furthermore, the choice of balance is the key to improving model accuracy, ~~such~~ as shown by the result of the RFRK-SBP3 model (Fig. 4). We also fitted the biplots using a random sampling test (70~~ %~~% of the soil ~~sampling~~ data was randomly sampled), and the ~~distribution~~ distributions (angle) of these graphs ~~(angle)~~ were almost the same (Fig. S3.1). Multiple data sets should be considered in further ~~researches~~studies to verify if ~~it was~~this is a general feature of soil ~~PSFs~~PSF samples or if it was produced from our data set.

~~Also, the~~The weighting problem was not considered in this study, because the ILR method can be qualified as an unweighted log-ratio transformation, giving all parts the same weight for both the definition of the total variance and the reduction of dimension. ~~It~~This may enlarge the ratios generated from the rare parts~~ and~~, which would dominate the analysis (Greenacre and Lewi, 2009). The pairwise log-ratio can be used to set weights by their proportions when there is no additional knowledge about the component measurement errors (Greenacre, 2019). Nevertheless, all three parts of the soil PSF data ~~dominate~~dominated the biplot diagram, without the influence of rare ~~element~~elements and with no redundancy; thus, ~~there are~~ ~~no~~none of the shortcomings mentioned above~~, and the accuracy~~ were apparent. Accuracy assessments using a pairwise log-ratio transformation ~~need more research~~require further study in the future.

4.3 Limitations

In this work, we used ILR transformation to demonstrate the correlation of soil PSF data, and different balances were also compared. However, these models were predicted separately for each ILR component (ILR1 and ILR2), which were suboptimal because they cannot further consider the cross correlations among ILR coordinates. In our pervious study, we have used compositional kriging (CK) for the spatial prediction of soil PSFs (Wang and Shi, 2017), and the cross correlations of

ILRs can be taken into account using CK. Although it is optimal, it cannot consider different balances of ILR, nor can it be combined with the hybrid interpolator (e.g., RK). Moreover, predicting each ILR component separately was a more suitable approach for the spatial prediction models currently used (such as the GLM and RF). Therefore, more alternative spatial prediction models combined with interpretation of ILR balances for compositional data should be considered in the future. For example, CK and high accuracy surface modelling (HASM; Yue et al., 2016) can be applied for small scale study areas. For large scale study areas, multivariate RF (Segal and Xiao, 2011) can be combined with a log-ratio transformation and hybrid interpolation, enabling the cross correlations among ILR coordinates to be better interpreted.

5 Conclusions

We evaluated and compared the performance of the GLM, RF, and their hybrid pattern (i.e., GLMRK and RFRK) using different ~~ILR~~ balances of ILR transformed data. The bias of the GLM was lower than ~~those~~that of the RF; however, the accuracy of the GLM was relatively ~~lower~~low. More discrete distributions and broader ranges of prediction value distributions were produced from GLMs in the USDA soil texture triangles. In other words, different data sets were generated from the use of the GLM and RF~~—~~, with unbiased and inaccurate predictions for the GLM and biased and more accurate predictions for the RF.

~~—~~The hybrid ~~patterns~~pattern of GLM and RF~~,~~ (i.e., RK~~, were recommended, which~~) was found to be the best solution because it produced ~~relative higher~~a relatively high prediction accuracy and ~~environmental correlation, showing~~strong correlations with ECs, providing more details about the soil sampling points (hot spots and cold spots) compared with only the regression ~~part~~model. However, the non-normal distribution of ILR transformed data, and the “black box” effect of the RF algorithm were drawbacks in the use of the GLMRK and RFRK.

~~Concerning~~For the different SBP balances~~ of SBP,~~, the three SBP-based data generated slightly different distributions~~. A slight difference was produced, and the~~, but no pattern was ~~not visible, which was~~ apparent. This could be explained ~~from~~by the angle of the biplot diagram~~—~~, with three rays of soil ~~PSFs~~PSF components clustered into three modes, and each part ~~dominated in~~dominating its cluster. Using the most abundant component of ~~compositions~~the compositional data as the first component of the permutations was not considered the right choice because ~~of~~SBP2 produced the worst performance~~ of SBP2. On the contrary~~. Instead, we ~~recommended~~recommend using other parts that ~~were~~are not the most abundant as the first component of permutations~~ when the biplot diagram was~~, which in this case resulted in a uniform distribution ~~with~~ on the biplot diagram, with a cluster at about 120~~°, like~~°. To consider the ~~form of our study. For a~~ general ~~feature~~features of soil ~~PSFs~~PSF compositional data, multiple soil ~~PSFs~~PSF data sets should be considered and compared in the future. This study can provide a reference for the spatial simulation of soil PSFs combined with ~~environmental covariables~~ECs at ~~a~~the regional scale, and how to choose the balances of ILR transformed data.

Data Availability. We did not use any new data and the data we used come from previously published sources. Soil particle-size fractions data is available through our previous studies (Wang and Shi, 2017, 2018). Moreover, it also can be visited on this website: http://data.tpdc.ac.cn/zh-hans/data/7f91d36d-8bbd-40d5-8eaf-7c035e742f40/ (Digital soil mapping dataset of soil texture (soil particle-size fractions) in the upstream of the Heihe river basin (2012-2016); last access: 4 July 2020). The meteorological data can be accessed through http://data.cma.cn/ (last access: 4 July 2020). Environmental covariates data of soil physical and chemical properties and categorical maps can be obtained through http://data.tpdc.ac.cn/zh-hans/ (last access: 4 July 2020), including saturated water content, field water holding capacity, wilt water content, saturated hydraulic conductivity data (http://data.tpdc.ac.cn/zh-hans/data/e977f5e8-972b-42a5-bffe-cd0195f3b42b/, Digital soil mapping dataset of hydrological parameters in the Heihe River Basin (2012); last access: 4 July 2020), and soil thickness data (http://data.tpdc.ac.cn/zh-hans/data/fc84083e-8c66-4a42-b729-4f19334d0d67/, Digital soil mapping dataset of soil depth in the Heihe River Basin (2012-2014); last access: 4 July 2020). DEM data set is provided by the Geospatial Data Cloud site, Computer Network Information Center, Chinese Academy of Sciences. (http://www.gscloud.cn, last access: 4 July 2020).

Author contribution. Wenjiao Shi contributed to soil data sampling, oversaw the design of the entire project. Mo Zhang performed the model analysis and wrote the manuscript. Both authors contributed to writing this paper and interpreting data.

Competing interests. The authors declare that they have no conflict of interest.

Acknowledgment. Our team expresses gratitude to the following institutions, Key Laboratory of Land Surface Pattern and Simulation, Institute of Geographic Sciences and Natural Resources Research, Chinese Academy of Sciences; School of Earth Sciences and Resources, China University of Geosciences; College of Resources and Environment, University of Chinese Academy of Sciences. This study was supported by the National Key Research and Development Program of China (No. 2017YFA0604703), the National Natural Science Foundation of China (Grant No. 41771111 and 41771364), Fund for Excellent Young Talents in Institute of Geographic Sciences and Natural Resources Research, Chinese Academy of Sciences (2016RC201), and the Youth Innovation Promotion Association, CAS (No. 2018071).

References

Aitchison, J.: The statistical analysis of compositional data, Chapman and Hall, Ltd., 416 pp., 1986.

Akpa, S. I. C., Odeh, I. O. A., Bishop, T. F. A., and Hartemink, A. E.: Digital mapping of soil particle-size fractions for Nigeria, Soil Sci. Soc. Am. J., 78, 1953-1966, https://doi.org/10.2136/sssaj2014.05.0202, 2014.

Beven, K. J., and Kirkby, M. J.: A physically based, variable contributing area model of basin hydrology / Un modèle à base physique de zone d'appel variable de l'hydrologie du bassin versant, Hydrological Sciences Bulletin, 24, 43-69, https://doi.org/10.1080/02626667909491834, 1979.

Bishop, T. F. A., and McBratney, A. B.: A comparison of prediction methods for the creation of field-extent soil property maps, Geoderma, 103, 149-160, https://doi.org/10.1016/S0016-7061(01)00074-X, 2001.

Breiman, L.: Bagging predictors, Machine Learning, 24, 123-140, https://doi.org/10.1023/a:1018054314350, 1996.

Breiman, L.: Random forests, Machine Learning, 45, 5-32, https://doi.org/10.1023/a:1010933404324, 2001.

Buchanan, S., Triantafilis, J., Odeh, I. O. A., and Subansinghe, R.: Digital soil mapping of compositional particle-size fractions using proximal and remotely sensed ancillary data, Geophysics, 77, WB201-WB211, https://doi.org/10.1190/geo2012-0053.1, 2012.

Conrad, O., Bechtel, B., Bock, M., Dietrich, H., Fischer, E., Gerlitz, L., Wehberg, J., Wichmann, V., and Böhner, J.: System for automated geoscientific analyses (SAGA) v. 2.1.4, Geosci. Model Dev., 8, 1991-2007, https://doi.org/10.5194/gmd-8-1991-2015, 2015.

D. Moore, I., K. Turner, A., Wilson, J., K. Jenson, S., and Band, L.: GIS and land-surface-subsurface process modeling, 196-230, 1993.

Delbari, M., Afrasiab, P., and Loiskandl, W.: Geostatistical analysis of soil texture fractions on the field scale, Soil and Water Research, 6, 173-189, https://doi.org/10.17221/9/2010-SWR, 2011.

Egozcue, J. J., Pawlowsky-Glahn, V., Mateu-Figueras, G., and Barcelo-Vidal, C.: Isometric logratio transformations for compositional data analysis, Mathematical Geology, 35, 279-300, https://doi.org/10.1023/a:1023818214614, 2003.

Egozcue, J. J., and Pawlowsky-Glahn, V.: Groups of parts and their balances in compositional data analysis, Mathematical Geology, 37, 795-828, https://doi.org/10.1007/s11004-005-7381-9, 2005.

Filzmoser, P., and Hron, K.: Correlation analysis for compositional data, Math Geosci., 41, 905-919, https://doi.org/10.1007/s11004-008-9196-y, 2009.

Filzmoser, P., Hron, K., and Reimann, C.: Univariate statistical analysis of environmental (compositional) data: Problems and possibilities, Sci. Total Environ., 407, 6100-6108, https://doi.org/10.1016/j.scitotenv.2009.08.008, 2009.

Fiserova, E., and Hron, K.: On the interpretation of orthonormal coordinates for compositional data, Math Geosci., 43, 455-468, https://doi.org/10.1007/s11004-011-9333-x, 2011.

Florinsky, I. V.: Accuracy of local topographic variables derived from digital elevation models, International Journal of Geographical Information Science, 12, 47-62, https://doi.org/10.1080/136588198242003, 1998.

Gallant, J. C., and Dowling, T. I.: A multiresolution index of valley bottom flatness for mapping depositional areas, Water Resources Research, 39, https://doi.org/10.1029/2002wr001426, 2003.

Goovaerts, P.: Geostatistics in soil science: state-of-the-art and perspectives, Geoderma, 89, 1-45, https://doi.org/10.1016/S0016-7061(98)00078-0, 1999.

Greenacre, M., and Lewi, P.: Distributional equivalence and subcompositional coherence in the analysis of compositional data, contingency tables and ratio-scale measurements, Journal of Classification, 26, 29-54, https://doi.org/10.1007/s00357-009-9027-y, 2009.

Greenacre, M.: variable selection in compositional data analysis using pairwise logratios, Math Geosci., 51, 649-682, https://doi.org/10.1007/s11004-018-9754-x, 2019.

Grimm, R., Behrens, T., Märker, M., and Elsenbeer, H.: Soil organic carbon concentrations and stocks on Barro Colorado

Island – Digital soil mapping using Random Forests analysis, Geoderma, 146, 102-113, https://doi.org/10.1016/j.geoderma.2008.05.008, 2008.

Hengl, T., Heuvelink, G. B. M., and Stein, A.: A generic framework for spatial prediction of soil variables based on regression-kriging, Geoderma, 120, 75-93, https://doi.org/10.1016/j.geoderma.2003.08.018, 2004.

Hengl, T., Heuvelink, G. B. M., Kempen, B., Leenaars, J. G. B., Walsh, M. G., Shepherd, K. D., Sila, A., MacMillan, R. A., de Jesus, J. M., Tamene, L., and Tondoh, J. E.: Mapping soil properties of Africa at 250 m resolution: random forests significantly improve current predictions, Plos One, 10, 26, https://doi.org/10.1371/journal.pone.0125814, 2015.

Hengl, T., Mendes de Jesus, J., Heuvelink, G. B. M., Ruiperez Gonzalez, M., Kilibarda, M., Blagotić, A., Shangguan, W., Wright, M. N., Geng, X., Bauer-Marschallinger, B., Guevara, M. A., Vargas, R., MacMillan, R. A., Batjes, N. H., Leenaars, J. G. B., Ribeiro, E., Wheeler, I., Mantel, S., and Kempen, B.: SoilGrids250m: Global gridded soil information based on machine learning, Plos One, 12, e0169748, https://doi.org/10.1371/journal.pone.0169748, 2017.

Hiemstra, P. H., Pebesma, E. J., Twenhöfel, C. J. W., and Heuvelink, G. B. M.: Real-time automatic interpolation of ambient gamma dose rates from the Dutch radioactivity monitoring network, Computers & Geosciences, 35, 1711-1721, https://doi.org/10.1016/j.cageo.2008.10.011, 2009.

K. Gerald van den Boogaart, and Raimon Tolosana, M. B.: Compositions: compositional data analysis, R package version 1.40-1 ed., available at: https://cran.rstudio.com/web/packages/compositions/index.html (last access: 14 July 2020), 2014.

Lane, P. W.: Generalized linear models in soil science, European Journal of Soil Science, 53, 241-251, https://doi.org/10.1046/j.1365-2389.2002.00440.x, 2002.

Lark, R. M.: A comparison of some robust estimators of the variogram for use in soil survey, European Journal of Soil Science, 51, 137-157, https://doi.org/10.1046/j.1365-2389.2000.00280.x, 2000.

Lark, R. M.: Two robust estimators of the cross-variogram for multivariate geostatistical analysis of soil properties, European Journal of Soil Science, 54, 187-201, https://doi.org/10.1046/j.1365-2389.2003.00506.x, 2003.

Lark, R. M., and Bishop, T. F. A.: Cokriging particle size fractions of the soil, Eur. J. Soil Sci., 58, 763-774, https://doi.org/10.1111/j.1365-2389.2006.00866.x, 2007.

Liaw, A., and Wiener, M.: Classification and regression by random forest, 23, available at: https://cran.r-project.org/web/packages/randomForest/index.html (last access: 14 July 2020), 2001.

Ließ, M., Glaser, B., and Huwe, B.: Uncertainty in the spatial prediction of soil texture: Comparison of regression tree and Random Forest models, Geoderma, 170, 70–79, https://doi.org/10.1016/j.geoderma.2011.10.010, 2012.

Lloyd, C. D., Pawlowsky-Glahn, V., and Jose Egozcue, J.: Compositional data analysis in population studies, Annals of the Association of American Geographers, 102, 1251-1266, https://doi.org/10.1080/00045608.2011.652855, 2012.

Martins, A. B. T., Bonat, W. H., and Ribeiro, P. J.: Likelihood analysis for a class of spatial geostatistical compositional models, Spat. Stat., 17, 121-130, https://doi.org/10.1016/j.spasta.2016.06.008, 2016.

Max Kuhn: Caret: Classification and regression training, R package version 6.0-80 ed., available at: https://cran.r-project.org/web/packages/caret/index.html (last access: 14 July 2020), 2018.

McBratney, A. B., Minasny, B., Cattle, S. R., and Vervoort, R. W.: From pedotransfer functions to soil inference systems, Geoderma, 109, 41-73, https://doi.org/10.1016/S0016-7061(02)00139-8, 2002.

McBratney, A. B., Santos, M. L. M., and Minasny, B.: On digital soil mapping, Geoderma, 117, 3-52, https://doi.org/10.1016/s0016-7061(03)00223-4, 2003.

Menafoglio, A., Guadagnini, A., and Secchi, P.: A kriging approach based on Aitchison geometry for the characterization of particle-size curves in heterogeneous aquifers, Stochastic Environmental Research and Risk Assessment, 28, 1835-1851, https://doi.org/10.1007/s00477-014-0849-8, 2014.

Menafoglio, A., Guadagnini, A., and Secchi, P.: A kriging approach based on Aitchison geometry for the characterization of particle-size curves in heterogeneous aquifers, Stoch. Environ. Res. Risk Assess., 28, 1835-1851, https://doi.org/10.1007/s00477-014-0849-8, 2014.

Menafoglio, A., Secchi, P., and Guadagnini, A.: A class-kriging predictor for functional compositions with application to particle-size curves in heterogeneous aquifers, Math Geosci., 48, 463-485, https://doi.org/10.1007/s11004-015-9625-7, 2016a.

Menafoglio, A., Guadagnini, A., and Secchi, P.: Stochastic simulation of soil particle-size curves in heterogeneous aquifer systems through a Bayes space approach, Water Resources Research, 52, 5708-5726, https://doi.org/10.1002/2015wr018369, 2016b.

Molayemat, H., Torab, F. M., Pawlowsky-Glahn, V., Morshedy, A. H., and Jose Egozcue, J.: The impact of the compositional nature of data on coal reserve evaluation, a case study in Parvadeh IV coal deposit, Central Iran, International Journal of Coal Geology, 188, 94-111, https://doi.org/10.1016/j.coal.2018.02.003, 2018.

Nelder, J. A., and Wedderburn, R. W. M.: Generalized linear models, Journal of the Royal Statistical Society. Series A (General), 135, 370-384, https://doi.org/10.2307/2344614, 1972.

Nickel, S., Hertel, A., Pesch, R., Schroeder, W., Steinnes, E., and Uggerud, H. T.: Modelling and mapping spatio-temporal trends of heavy metal accumulation in moss and natural surface soil monitored 1990-2010 throughout Norway by multivariate generalized linear models and geostatistics, Atmospheric Environment, 99, 85-93, https://doi.org/10.1016/j.atmosenv.2014.09.059, 2014.

Odeh, I. O. A., McBratney, A. B., and Chittleborough, D. J.: Further results on prediction of soil properties from terrain attributes: heterotopic cokriging and regression-kriging, Geoderma, 67, 215-226, https://doi.org/10.1016/0016-7061(95)00007-B, 1995.

Pawlowsky-Glahn, V.: On spurious spatial covariance between variables of constant sum, 107-113 pp., 1984.

Pawlowsky-Glahn V, Egozcue JJ, Tolosana-Delgado R.: Modeling and analysis of compositional data. John Wiley & Sons, Ltd, 2015.

R Development Core Team: R: A language and environment for statistical computing, in, R Foundation for Statistical Computing, Vienna, Austria, 2019.

Scarpone, C., Schmidt, M. G., Bulmer, C. E., and Knudby, A.: Modelling soil thickness in the critical zone for Southern British

Columbia, Geoderma, 282, 59-69, https://doi.org/10.1016/j.geoderma.2016.07.012, 2016.
Segal, M. and Xiao, Y. Y.: Multivariate random forests,Wiley Interdisciplinary Reviews-Data Mining and Knowledge Discovery, 1, 80–87, https://doi.org/10.1002/widm.12, 2011.
Song, X.-D., Brus, D. J., Liu, F., Li, D.-C., Zhao, Y.-G., Yang, J.-L., and Zhang, G.-L.: Mapping soil organic carbon content by geographically weighted regression: A case study in the Heihe River Basin, China, Geoderma, 261, 11-22, https://doi.org/10.1016/j.geoderma.2015.06.024, 2016.
Talska, R., Menafoglio, A., Machalova, J., Hron, K., and Fiserova, E.: Compositional regression with functional response, Computational Statistics & Data Analysis, 123, 66-85, 10.1016/j.csda.2018.01.018, 2018.
Tolosana-Delgado, R., Otero, N., Pawlowsky-Glahn, V., and Soler, A.: Latent compositional factors in the Llobregat River Basin (Spain) hydrogeochemistry, Mathematical Geology, 37, 681-702, https://doi.org/10.1007/s11004-005-7375-7, 2005.
Venables, W. N., and Dichmont, C. M.: GLMs, GAMs and GLMMs: an overview of theory for applications in fisheries research, Fisheries Research, 70, 319-337, https://doi.org/10.1016/j.fishres.2004.08.011, 2004.
Walvoort, D. J. J., and de Gruijter, J. J.: Compositional Kriging: A spatial interpolation method for compositional data, Mathematical Geology, 33, 951-966, https://doi.org/10.1023/a:1012250107121, 2001.
Wang, Z., and Shi, W. J.: Mapping soil particle-size fractions: A comparison of compositional kriging and log-ratio kriging, J. Hydrol., 546, 526-541, https://doi.org/10.1016/j.jhydrol.2017.01.029, 2017.
Wang, Z., and Shi, W. J.: Robust variogram estimation combined with isometric log-ratio transformation for improved accuracy of soil particle-size fraction mapping, Geoderma, 324, 56-66, https://doi.org/10.1016/j.geoderma.2018.03.007, 2018.
Yang, R.-M., Zhang, G.-L., Liu, F., Lu, Y.-Y., Yang, F., Yang, F., Yang, M., Zhao, Y.-G., and Li, D.-C.: Comparison of boosted regression tree and random forest models for mapping topsoil organic carbon concentration in an alpine ecosystem, Ecological Indicators, 60, 870-878, https://doi.org/10.1016/j.ecolind.2015.08.036, 2016.
Yi, C., Li, D., Zhang, G., Zhao, Y., Yang, J., Liu, F., and Song, X.: Criteria for partition of soil thickness and case studies, Acta Pedologica Sinica, 52, 220-227, 2015.
Yue, T., Liu, Y., Zhao, M., Du, Z., and Zhao, N.: A fundamental theorem of Earth's surface modelling, Environ. Earth Sci., 75, 751, https://doi.org/10.1007/s12665-016-5310-5, 2016.
Yue, T., Zhao, N., Liu, Y., Wang, Y., Zhang, B., Du, Z., Fan, Z., Shi, W., Chen, C., Zhao, M., Song, D., Wang, S., Song, Y., Yan, C., Li, Q., Sun, X., Zhang, L., Tian, Y., Wang, W., Wang, Y. a., Ma, S., Huang, H., Lu, Y., Wang, Q., Wang, C., Wang, Y., Lu, M., Zhou, W., Liu, Y., Wang, Z., Bao, Z., Zhao, M., Zhao, Y., Rao, Y., Naseer, U., Fan, B., Li, S., Yang, Y., and Wilson, J. P.: A fundamental theorem for eco-environmental surface modelling and its applications, Science China-Earth Sciences, 63, 1092-1112, https://doi.org/10.1007/s11430-019-9594-3, 2020.
Zhang, M., Shi, W., and Xu, Z.: Systematic comparison of five machine-learning models in classification and interpolation of soil particle size fractions using different transformed data, Hydrol. Earth Syst. Sci., 24, 2505-2526, https://doi.org/10.5194/hess-24-2505-2020, 2020.